PROCEEDINGS OF SCIENCE

# Search for pair- and single-production of vector-like quarks in final states with at least one $Z$ boson decaying into a pair of electrons or muons in $pp$ collision data collected with the ATLAS detector at $\sqrt{s} = 13$ TeV

**Elena Freundlich***[†]**, On behalf of the ATLAS Collaboration**
*Technische Universität Dortmund*
*E-mail:* elena.freundlich@cern.ch

A search for pair- and single-production of vector-like quarks $T$ and $B$ with a leptonically decaying $Z$ boson is presented. The data were collected in $pp$ collisions at $\sqrt{s} = 13$ TeV with the ATLAS detector at the LHC, corresponding to an integrated luminosity of 36.1 fb$^{-1}$. Final states are required to contain a $Z$ boson reconstructed from a same-flavor pair of leptons with opposite electric charge and a third generation quark. The analysis targets both pair- and single-production of vector-like quarks and no excess above the Standard Model expectation is found. Lower mass limits on vector-like $T$ and $B$ quarks at 95% confidence level are derived and limits on the coupling to Standard Model quarks are set for single-production.

*Sixth Annual Conference on Large Hadron Collider Physics (LHCP 2018)*
*4-9 June 2018*
*Bologna, Italy*

*Speaker.
[†]This work is supported by the Konrad-Adenauer-Stiftung.




PoS(LHCP2018)017

## 1. Introduction

When searching for physics beyond the Standard Model (SM), Composite Higgs [1, 2] and Little Higgs [3, 4] models play an important role. These models predict vector-like quarks, whose right- and left-handed parts have the same transformation properties with respect to the weak isospin group SU(2). This analysis [5] at the ATLAS experiment [6] at the LHC focuses on the search for pair- and single-production of vector-like $T$ and $B$ quarks with charges $q_T = \frac{2}{3}e$ and $q_B = -\frac{1}{3}e$. For the vector-like quark decays the assumption is made that only decays to a $W$, $Z$ or $H$ boson and a third generation quark are possible. The final state is required to contain a $Z$ boson reconstructed from a lepton pair $\ell^+\ell^-$ ($\ell = e, \mu$). Figure 1 shows Feynman diagrams for both processes under study, one mediated by the weak and one by the strong force.

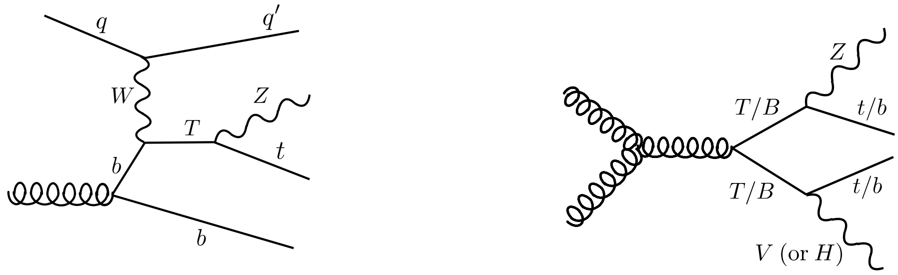


Figure 1: Feynman diagrams for single-production (left) and pair-production (right) of vector-like quarks with at least one $Z$ boson in the final state.

## 2. Analysis strategy

The final states presented in Figure 1 contain different multiplicities of leptons, large-$R$ jets with radius $R = 1.0$, $b$-tagged small-$R$ jets with $R = 0.4$ and high-$p_{\mathrm{T}}$ objects alongside other discriminating features.

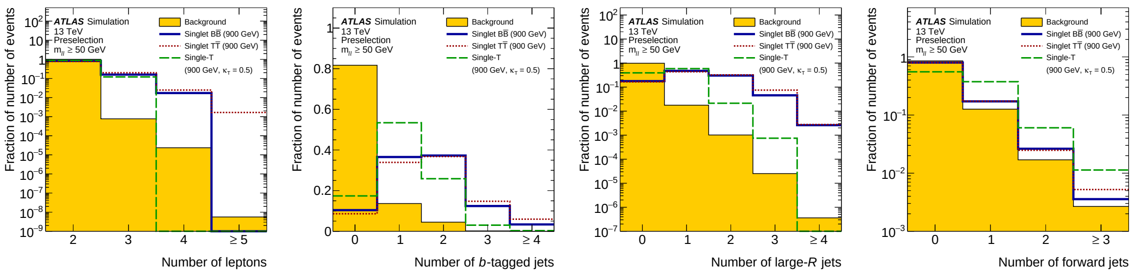


Figure 2: Normalized distributions of the lepton multiplicity, the number of $b$-tagged jets, the large-$R$ jet multiplicity and the forward jet multiplicity (from left to right) [5].

Figure 2 shows the distributions used for splitting the analysis into three orthogonal channels for pair-production, while there are two different channels for single-production. Channels with two leptons have a higher signal efficiency, while the background rejection is better for channels with at least three leptons. A requirement of at least one $b$-tagged small-$R$ jet rejects a lot of background and can be extended to at least two for channels with a large number of events. Furthermore, the number of large-$R$ jets discriminates well between signal and background and is used in the pair-production (PP) dilepton ($2\ell$) channels. For the single-production channels, the number of forward jets is required to be at least one, removing a substantial amount of background. To summarize, five different channels are defined: These are PP $2\ell$ with $\leq 1$ large-$R$ jet or $\geq 2$ large-R jets, PP $\geq 3\ell$, and for single-production (SP) $2\ell$ and $\geq 3\ell$. The main backgrounds are $Z$+jets (PP $2\ell$ 0-1J, PP $2\ell$ 2J, SP $2\ell$), $t\bar{t}$ (PP $2\ell$ 0-1J, PP $2\ell$ 2J), $t\bar{t}+X$ (PP $2\ell$ 2J, PP $\geq 3\ell$, SP $2\ell$, SP $\geq 3\ell$) and diboson events (PP $\geq 3\ell$, SP $2\ell$, SP $\geq 3\ell$).

Five channels are optimized individually and a final discriminant is chosen. Either the reconstructed vector-like quark mass $m_{Zb}$ or $m_{Zt}$ or a scalar sum of object momenta is chosen ($H_{\mathrm{T}}$ for jets and $S_{\mathrm{T}}$ for leptons+jets). In Figure 3 and Figure 4 the final discriminants for each channel are illustrated. Data and Monte Carlo expectation agree well within the uncertainties.

Each discriminant is used in a statistical analysis in order to test for a discovery or set limits on the vector-like quark mass or the production cross-section times branching ratio $\sigma \times BR$. For the statistical analysis a binned profile likelihood fit is used based on the $CL_s$ method.

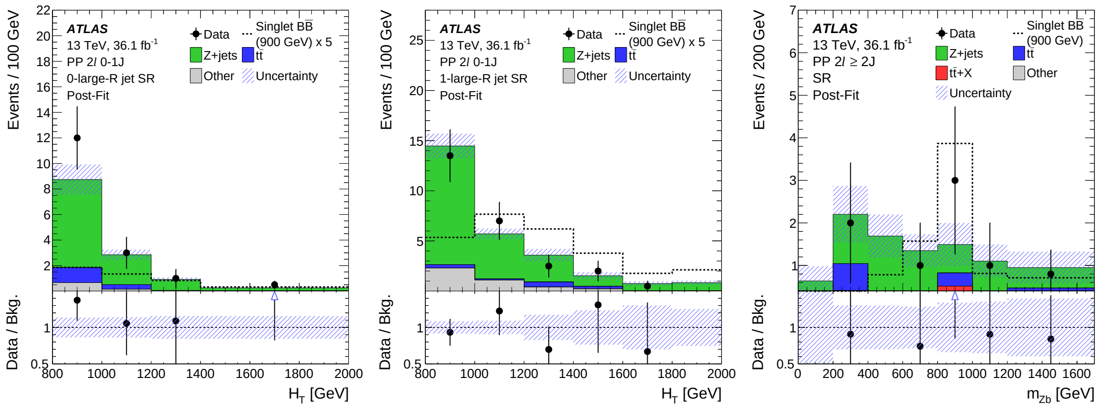


Figure 3: Final discriminants for the PP $2\ell$ channels showing $H_T$ (left and center) and $m_{Zb}$ (right) [5].

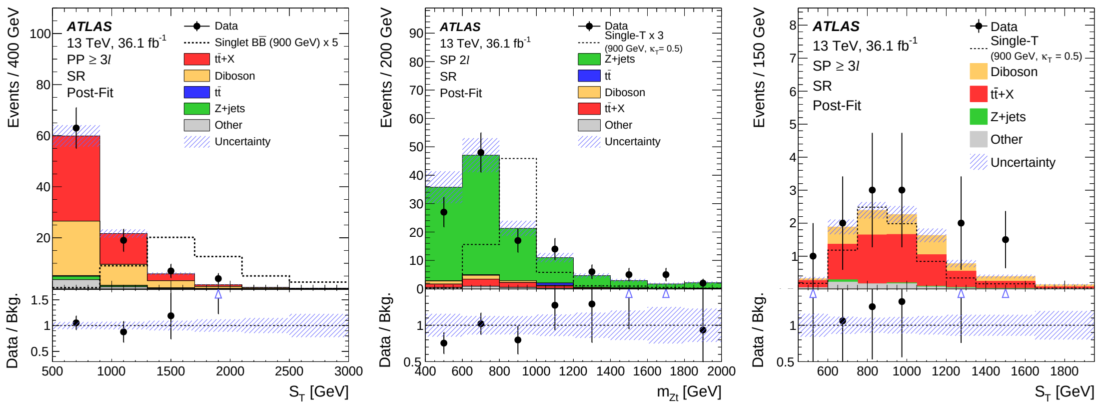


Figure 4: Final discriminants for the PP $\geq 3\ell$ channel (left) and for the single-production dilepton (center) and trilepton (right) channels [5].

## 3. Results

After performing the profile likelihood fit with all systematic uncertainties taken as nuisance parameters, no significant excess above the SM expectation is observed. Therefore, 95% confidence level (*CL*) limits are derived on $\sigma \times BR$ and the couplings to the SM quarks. In Table 5 the limits for PP are listed for the doublet models (with $BR(T/B \to t/b) = 50\%$).

Instead of focusing on a specific signal model the whole branching ratio plane can be scanned under the assumption that all *BR*s add up to one. Figure 6 shows this scan and clearly illustrates the largest sensitivity in the *Z* corner.

| Model | $2\ell$ 0-1J exp. | $2\ell \geq$ 2J exp. | $\geq 3\ell$ exp. | Combination obs. (exp.) |
|---|---|---|---|---|
| $T\bar{T}$ doublet | 820 GeV | 1100 GeV | 1150 GeV | 1210 (1210) GeV |
| $B\bar{B}$ doublet | 1000 GeV | 1070 GeV | 880 GeV | 1140 (1120) GeV |

Figure 5: Expected exclusion limits on the vector-like quark *T* or *B* masses for each individual channel. Expected and observed limits are shown for the combination [5].

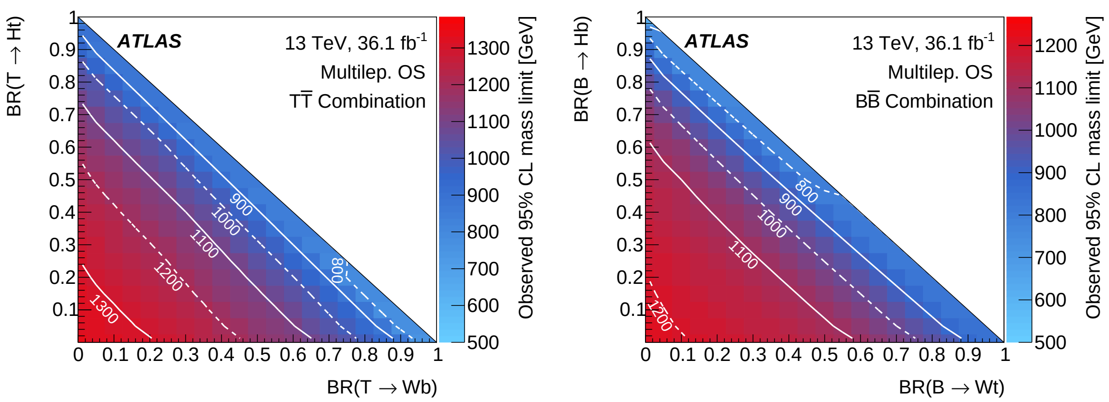


Figure 6: Two-dimensional limits in the branching ratio plane for vector-like *T* (left) and *B* (right) showing the PP combination limits [5].

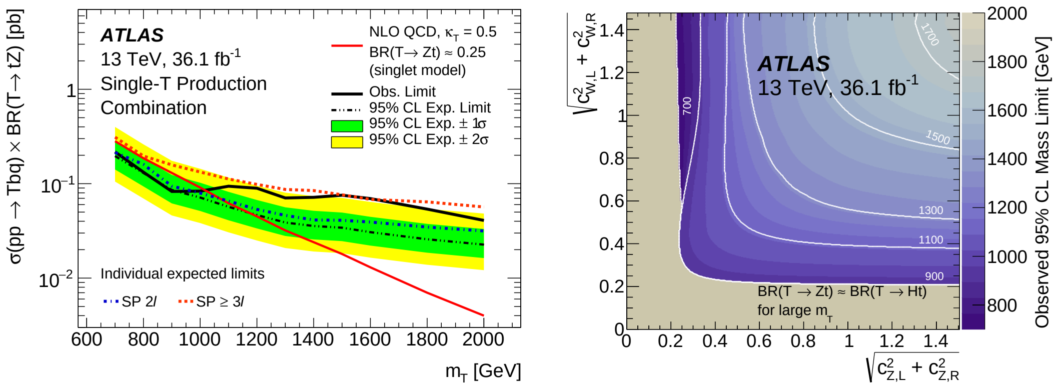


Figure 7: Expected and observed 95% *CL* limits on $\sigma \times BR$ depending on the vector-like *T* mass $m_T$ for the individual SP channels and their combination for a coupling of $\kappa_T = 0.5$ [7] (left). Observed lower limits on $m_T$ for SP combination as a function of the coupling $c_W$ and $c_Z$ (in the high-$m_T$ limit) [5] (right).

For single-production 95% *CL* limits are set on $\sigma \times BR$ with a nominal coupling $\kappa_T = 0.5$ introduced in the model in Ref. [7]. In Figure 7 the limits are shown for both SP channels and their combination. The value of $\kappa_{\mathrm{T}} = 0.5$ corresponds to $c_W = \sqrt{c_{L,W}^2 + c_{R,W}^2} = 0.45$, a coupling in another model from Ref. [8]. The coupling $c_W$ can then be reinterpreted in terms of a mixing angle $|\sin(\Theta_L)|$ [9] between $T$ and the SM top quark. In Figure 8 (left) the exclusion of the $c_W$ parameter space depending on the vector-like $T$ mass $m_T$ is shown for the singlet model. All values above the observed limit are excluded. For the mixing angle interpretation in Figure 8 (right) mixing angles within the contour are excluded. Furthermore, more generalized limits are set in coupling-mass space by assuming $BR(T \to Zt) \approx BR(T \to Ht)$ in the high-mass limit $m_T$. Subsequently, $T$ masses as a function of the coupling to $W$, $Z$ and $H$ can be excluded. The corresponding exclusion limit plot can be seen in Figure 7 (right).

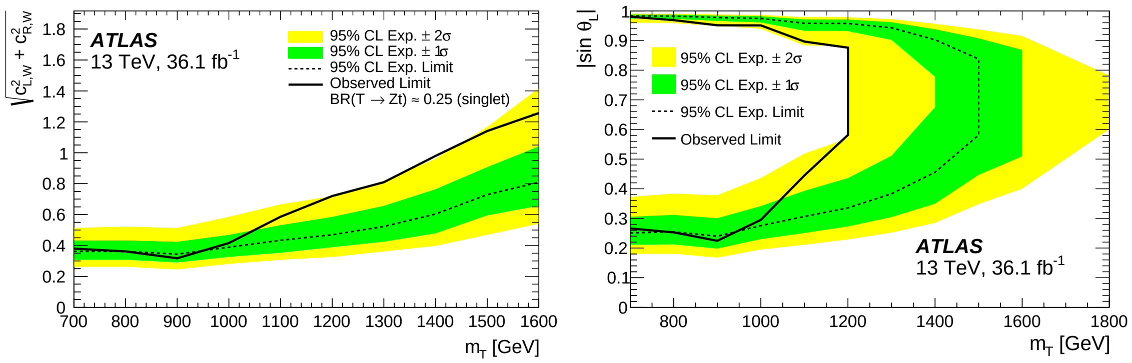


Figure 8: Expected and observed 95% $CL$ limits for the SP combination on the coupling $c_W$ of $T$ to SM particles in the singlet model (left) and on the mixing angle $|\sin(\Theta_L)|$ [5].

## 4. Conclusion

A search for vector-like $T$ (in pair- and single-production) and $B$ quarks (in pair-production) was presented with data collected at the ATLAS experiment at the LHC. No excess above the SM expectation was found and limits on $\sigma \times BR$ as well as different couplings and mixing angles could be set. The large number of high-$p_{\mathrm{T}}$ objects motivate the use of boosted techniques like large-$R$ jets. Single and pair-production channels were combined, increasing the overall sensitivity.

## References


[1] D. B. Kaplan, H. Georgi, and S. Dimopoulos, *Composite Higgs scalars*, Phys. Lett. B **136** (1984) 187.

[2] K. Agashe, R. Contino, and A. Pomarol, *The minimal composite Higgs model*, Nucl. Phys. B **719** (2005) 165, arXiv: hep-ph/0412089.

[3] N. Arkani-Hamed, A. Cohen, E. Katz, and A. Nelson, *The Littlest Higgs*, JHEP **07** (2002) 34, arXiv: hep-ph/0206021.

[4] M. Schmaltz and D. Tucker-Smith, *LITTLE HIGGS THEORIES*, Ann. Rev. Nucl. Part. Sci. **55** (2005) 229, arXiv: hep-ph/0502182.

[5] ATLAS Collaboration, *Search for pair- and single-production of vector-like quarks in final states with at least one Z boson decaying into a pair of electrons or muons in pp collision data collected with the ATLAS detector at* $\sqrt{s} = 13$ *TeV*, (2018), arXiv: 1806.10555.

[6] ATLAS Collaboration, *The ATLAS Experiment at the CERN Large Hadron Collider*, JINST **3** (2008) S08003.

[7] M. Buchkremer, G. Cacciapaglia, A. Deandrea, and L. Panizzi, *Model-independent framework for searches of top partners*, Nucl. Phys. B **876** (2013) 376, arXiv: 1305.4172.

[8] O. Matsedonskyi, G. Panico, and A. Wulzer, *On the interpretation of Top Partners searches*, JHEP **12** (2014) 097, arXiv: 1409.0100.

[9] J. A. Aguilar-Saavedra, R. Benbrik, S. Heinemeyer, and M. Pérez-Victoria, *Handbook of vectorlike quarks: Mixing and single production*, Phys. Rev. D **88** (2013) 094010, arXiv: 1306.0572.